



A new species of the fish louse genus *Dipteropeltis* Calman, 1912 (Crustacea: Branchiura) from Peru

LYRA M. GABOARDI^{1*}, LAWRENCE E. REEVES², GERMÁN AUGUSTO MURRIETA MOREY³, DANIEL L. STANTON^{4,5} & RYAN M. CARNEY¹

¹Department of Integrative Biology, University of South Florida; 4202 E. Fowler Ave., Tampa, FL USA 33620.

✉ lyramgaboardi@gmail.com; <https://orcid.org/0009-0006-5573-242X>

✉ ryancarney@usf.edu; <https://orcid.org/0000-0002-5537-5366>

²UF/IFAS Florida Medical Entomology Lab, University of Florida; 200 9th St SE, Vero Beach, FL USA 32962.

✉ lereeves@ufl.edu; <https://orcid.org/0000-0003-3968-8124>

³Instituto de Investigaciones de la Amazonía Peruana, Av. Jose Abelardo Quiñones Km. 2.5, 00784, Iquitos, Peru 00784.

✉ gmurrieta@iiaap.gob.pe; <https://orcid.org/0000-0001-6244-2654>

⁴UF/IFAS Citrus Research and Education Center, University of Florida; 700 Experiment Station Rd. Lake Alfred, FL USA 33850.

✉ stantond2@ufl.edu; <https://orcid.org/0000-0003-3238-4523>

⁵Department of Animal Sciences, University of Florida; 2250 Shealy Dr. Gainesville, FL USA 32608.

*corresponding author

Abstract

Dipteropeltis is a poorly described genus of fish louse endemic to South America. In a small blackwater region within Loreto, Peru, 13 adult and juvenile specimens of an unidentified species of *Dipteropeltis* Calman, 1912, as well as one adult specimen of *D. hirundo* Calman, 1912, were observed and collected. Scanning electron and light micrographs were acquired to examine and measure key features of these specimens. Morphological differences from the two known species of *Dipteropeltis*, *D. hirundo* and *D. campanaformis* Neethling *et al.*, 2014, indicate that the collected specimens represent a new species. *Dipteropeltis longicaudatus* sp. nov. is diagnosed by elongate abdominal lobes, a chevron-shaped carapace, and uniquely shaped maxillae. One specimen represents the longest branchiuran documented to date at 31.5 mm. Additionally, we provide the first sequence data for this genus using DNA barcoding, which corroborates our designation of a new species. Videos were also captured that document behaviors including host attachment, pulsating abdominal lobes, suction disc “walking”, and swimming. Findings have implications for its teleost hosts, *Triportheus albus* Cope, 1872 and *Brycon amazonicus* Spix & Agassiz, 1829, the latter being a critical species for aquaculture and commercial fisheries in Amazonia.

Key words: Argulidae, *Brycon amazonicus*, DNA barcoding, ontogeny, parasite, scanning electron microscopy, South America, *Triportheus albus*

Introduction

Branchiura is a subclass of ectoparasitic crustaceans colloquially known as fish lice. It comprises a single family Argulidae with over 200 taxa in four described genera: *Argulus* Müller, 1792, *Chonopeltis* Thiele, 1900, *Dipteropeltis* Calman, 1912, and *Dolops* Audouin, 1837. While all genera have paired maxillulae which grip the host, *Dolops* retains an ancestral hook-like morphology, whereas the other three genera have maxillulae that evolved into a suction cup-like structure (Møller *et al.* 2008).

Dipteropeltis is the only genus within Argulidae endemic to South America and is known from that continent alone (Hadfield 2019). Currently, just two species have been described: *D. hirundo* and *D. campanaformis*. Both species have been observed in various locations in Brazil, including Boa Esperança, Manaus, and Corumba. *Dipteropeltis hirundo* has also been reported in Argentina (Weibezahn & Cobo 1964) and Venezuela (Ringuelet 1943). Morphological descriptions of *Dipteropeltis* are limited, with only adult females having been documented. The rarity and sex of these specimens may be due to the hypothesized nature of this genus being temporary parasites that only attach during feeding (Van As & Van As 2019). Indeed, unlike most other aquatic parasites, most branchiurans are able to swim freely throughout their entire life (Mikheev *et al.* 2015).

Presumably aided by this free-swimming ability, argulids switch hosts many times; they damage host tissues and contribute to host stress, all of which facilitate the transfer of pathogens (Mikheev *et al.* 2015). For example, *Argulus* spp. are known to spread nematode larvae and diseases such as carp pox and spring viraemia of carp, the latter of which has a high mortality rate and can cause severe economic consequences for the aquaculture industry (Molnár & Székely 1998; Moravec *et al.* 1999; Hadfield & Smit 2019). Similarly, such parasites can cause argulosis in their fish hosts, resulting in reduced growth and survival, and consequently increased production costs in commercial fisheries (Mikheev *et al.* 2015). All of this can be exacerbated by intensive fish farming practices and inbreeding depression, which can lead to increased virulence of and vulnerability to parasites (Mennerat *et al.* 2010; Smallbone *et al.* 2016). Fish lice can even reach high enough numbers to result in fish kills in aquaculture operations, aquaria, and more rarely the wild (Poly 2008).

Notably, *D. hirundo* infects *Brycon amazonicus*, which plays a critical role in subsistence and commercial fisheries as well as aquaculture (de Oliveira *et al.* 2018). Both the migratory nature of this fish, as well as its removal from the wild for aquaculture, could contribute to the dispersion of fish lice to new regions and populations. It should also be noted that *Dipteropeltis* spp. have so far been documented to infect at least 15 species across five families in two orders at a prevalence as high as 73% (herein; Neethling *et al.* 2014; Luque *et al.* 2013; Fontana *et al.* 2012; Mamani *et al.* 2004; Carvalho *et al.* 2003). Based on specimens collected from two species of characiform fish, here we characterize *Dipteropeltis longicaudatus* **sp. nov.** from Peru and use comparative morphological and molecular approaches which distinguish the specimens from *D. hirundo* and *D. campanaformis*.

Methods

Thirteen *Dipteropeltis* spp. specimens were obtained by pole fishing in the Tamshiyacu Tahuayo Reserve roughly 40 km south of Iquitos, Loreto, Peru (Fig. 1). All were collected within a 6 km stretch of the upper Tahuayo River, a blackwater Amazon tributary, between August 1–16, 2019. Specimens were collected at various times of the day (from dawn to nearly dusk) from *Brycon amazonicus*, locally known as “sábalo”, and *Tripurtheus albus*, locally known as “sardina” (Table 1). All collected hosts measured 15–25 cm in length. All specimens were collected under the authority of the Amazon Research Center, which is formally registered as an official research institution with Peru’s scientific council, Consejo Nacional de Ciencia, Tecnología e Innovación (CONCYTEC). Approval from an ethics committee and licenses for working with fish species were followed according to the following resolutions: No132-2014-GRL-DIREPRO, No21-2016 GRL-DIREPRO, and PTH-068-16-PECSANIPES.

Morphological differences among collected *D. longicaudatus* **sp. nov.** specimens were immediately apparent; thus, specimens were split into three groups for comparison. Seven specimens of the type series are larger and have longer abdominal lobes (Group I) compared to six other specimens (Group II). A third group was formed comprising one specimen that closely resembled *D. hirundo* descriptions from Møller & Olesen 2010. Specimens were observed attached to their hosts, then under a 20X stereo microscope with a static field of view of 1 cm. Specimens were preserved in 70% isopropyl alcohol. One specimen from Group II was lost during preservation and reallocation before measurements could be taken. Specimens were measured according to Neethling *et al.* 2014 (Table 1). Morphological measurements include abdomen length (AL), abdomen split length (ASL), carapace split length (CSL), distance from head to abdominal lobe end (HA), distance from head to carapace lobe end (HC), and sucker diameter (SD). Ratios of various measurements were also calculated to highlight the differences between groups I, II, and III.

Specimens I.4, I.7, and II.6 were chosen for SEM analysis and transferred to 70% ethanol. These specimens were rehydrated through a decreasing series of ethanol solutions (50%, 25%), rinsed with 1X PBS, and fixed in 4% paraformaldehyde in 1X PBS overnight at 4°C. Specimens were rinsed with 1X PBS and dehydrated in an ethanol series (30%, 50%, 70%, 80%, 85%, 95%, 100%; 3X) and critical point dried using a Ladd 2800 critical point dryer (Ladd Research Industries, Williston, VT, USA). Specimens were then mounted onto SEM stubs using a double-sided 12 mm carbon sticker (Electron Microscopy Sciences, Hatfield PA, USA), sputter coated with gold/palladium using a Ladd 30800 sputter coater (Ladd Research Industries), and observed and imaged using a Topcon Aquila compact SEM and optical microscope (Topcon Positioning Systems, Livermore, CA, USA).

Specimens I.1, II.4, and III.1 were chosen for DNA barcoding analysis, and results were compared to deposited samples in the Barcode of Life Data System (BOLD) managed by the Centre for Biodiversity Genomics (Ratnasingham & Hebert 2007). DNA was extracted using a Zymo Quick-DNA Miniprep Plus Kit (Genesee Scientific Corp., El

Cajon, CA). Extraction buffer was added to each tube, and the tissue was macerated with a sterile plastic pestle for approximately 3 min. Subsequent steps followed the manufacturer protocol with an overnight incubation at 56°C. Extracted DNA was used as a template in polymerase chain reactions (PCR) to amplify a 658 bp fragment of the barcoding region of the cytochrome c oxidase subunit I (COI) gene. The 20 µl reaction consisted of 10 µL 2X Apex Taq RED Master Mix (Genesee Scientific Corp., San Diego, CA), 2 µL of 10 µM forward primer LCO1490 (5'-GGT CAA CAA ATC ATA AAG ATA TTG G-3'; Folmer *et al.* 1994), 2 µL of 10 µM reverse primer HCO2198 (5'-TAA ACT TCA GGG TGA CCA AAA AAT CA-3; Folmer *et al.* 1994), 1 µL extracted DNA, and 5 µL sterile water. Reactions were performed in a BioRad T100 thermal cycler programmed to 94°C for 1 min; five cycles of 94°C for 30 sec, 45°C for 40 sec, and 72°C for 1 min; 35 cycles of 94°C for 30 sec, 51°C for 40 sec, and 72°C for 1 min; and a final extension step of 72°C for 10 min. After PCR, 7 µL of each PCR product were stained and electrophoresed on a 1.5% agarose gel alongside a 100 bp DNA ladder for 45 min at 50 V and examined under a transilluminator to verify that the amplicon was the expected size. A DNA ladder is a solution of DNA molecules of various known lengths, that when electrophoresed alongside PCR products, provides an estimate of the size of amplified DNA fragments through visual comparison with the reference DNA ladder fragments. An aliquot of amplicon was sent to Eurofins Genomics (Louisville, KY) for sequencing (Sanger *et al.* 1977).

DNA sequence chromatograms were visualized with the bioinformatic software Geneious Prime 2020.1.2 Version 11.0.6 (Biomatters, Inc., San Diego, CA). Each sequence was examined and edited for quality to remove ambiguous base calls before sequences were submitted to the BOLD v. 4 Identification Engine for taxonomic identification by alignment to reference COI sequences. Sequences from each group of our *Dipteropeltis* specimens collected in Peru were aligned to each other and to representative COI sequences from species of *Argulus*, *Chonopeltis*, and *Dolops* downloaded from the National Center for Biotechnology Information GenBank database. This alignment was created using the *Global alignment with free end gaps* tool within the Geneious Prime software. Sequences within the alignment were truncated so that all sequences were equal in length (533 bp). The aligned sequences were used to construct a neighbor-joining tree (Suppl. Fig. 1) with the Jukes-Cantor genetic distance model using the Geneious Tree Builder tool.



FIGURE 1. Samples were collected from the upper Tahuayo River within the Tamshiyacu Tahuayo Reserve in Peru. Within the black inset, the red box indicates the region where specimens were collected. Adult holotype (MUSM 5128, I.2) was collected at -4.394542, -73.264189. Inset scale bar = 2 km.

TABLE 1. Host species and morphological measurements for the 13 specimens collected. Groups correspond to *Dipteropeltis longicaudatus* sp. nov. adults (I) and juveniles (II), as well as *Dipteropeltis hirundo* (III). Specimen I.2 is the holotype (MUSM 5128). Specimen II.1 was found on host *Brycon amazonicus*; no measurements were taken before its loss. Gravid specimens denoted with asterisk (*). Measurements and ratios are based on Neethling *et al.* 2014: abdomen length (AL), abdomen split length (ASL), carapace split length (CSL), distance from head to abdominal lobe end (HA), distance from head to carapace lobe end (HC), and sucker diameter (SD). Units are in millimeters (mm).

Specimen ID	Host species	AL	ASL	CSL	HA	HC	SD	HC/HA	HA/HC	CSL/HC	ASL/AL	AL/HA	AL/HC	SD/HA	SD/HC
I.1*	<i>Triportheus albus</i>	11.3	10.4	6.3	19.0	9.5	1.0	0.50	2.00	0.66	0.92	0.59	1.19	0.05	0.11
I.2*	<i>Triportheus albus</i>	11.0	9.5	7.0	17.5	10.0	1.0	0.57	1.75	0.70	0.86	0.63	1.10	0.06	0.10
I.3	<i>Brycon amazonicus</i>	8.0	7.0	6.5	14.0	8.5	1.0	0.61	1.65	0.76	0.88	0.57	0.94	0.07	0.12
I.4*	<i>Triportheus albus</i>	22.0	20.5	12.5	31.5	16.0	1.0	0.51	1.97	0.78	0.93	0.70	1.38	0.03	0.06
I.5	<i>Brycon amazonicus</i>	12.5	10.5	5.5	19.5	7.5	0.8	0.38	2.60	0.73	0.84	0.64	1.67	0.04	0.10
I.6	<i>Brycon amazonicus</i>	7.0	6.5	5.0	11.0	7.5	0.8	0.68	1.47	0.67	0.93	0.64	0.93	0.07	0.10
I.7	<i>Triportheus albus</i>	7.0	5.5	5.0	13.0	7.5	0.8	0.58	1.73	0.67	0.79	0.54	0.93	0.06	0.10
II.2	<i>Brycon amazonicus</i>	1.5	1.3	1.5	4.5	3.0	0.5	0.67	1.50	0.50	0.83	0.33	0.50	0.11	0.17
II.3	<i>Brycon amazonicus</i>	1.5	1.0	2.0	5.0	3.5	0.5	0.70	1.43	0.57	0.67	0.30	0.43	0.10	0.14
II.4	<i>Brycon amazonicus</i>	0.8	0.5	0.8	3.0	2.0	0.3	0.67	1.50	0.38	0.67	0.25	0.38	0.08	0.13
II.5	<i>Brycon amazonicus</i>	1.3	1.0	2.0	4.5	3.3	0.5	0.72	1.38	0.62	0.80	0.28	0.38	0.11	0.15
II.6	<i>Triportheus albus</i>	1.0	0.8	1.0	3.5	2.5	0.5	0.71	1.40	0.40	0.75	0.29	0.40	0.14	0.20
III.1*	<i>Brycon amazonicus</i>	4.7	4.0	11.0	13.5	14.7	0.75	1.09	0.92	0.75	0.85	0.35	0.32	0.05	0.05

Results

Systematics

Subclass Branchiura Thorell, 1864

Order Arguloidea Yamaguti, 1963

Family Argulidae Leach, 1819

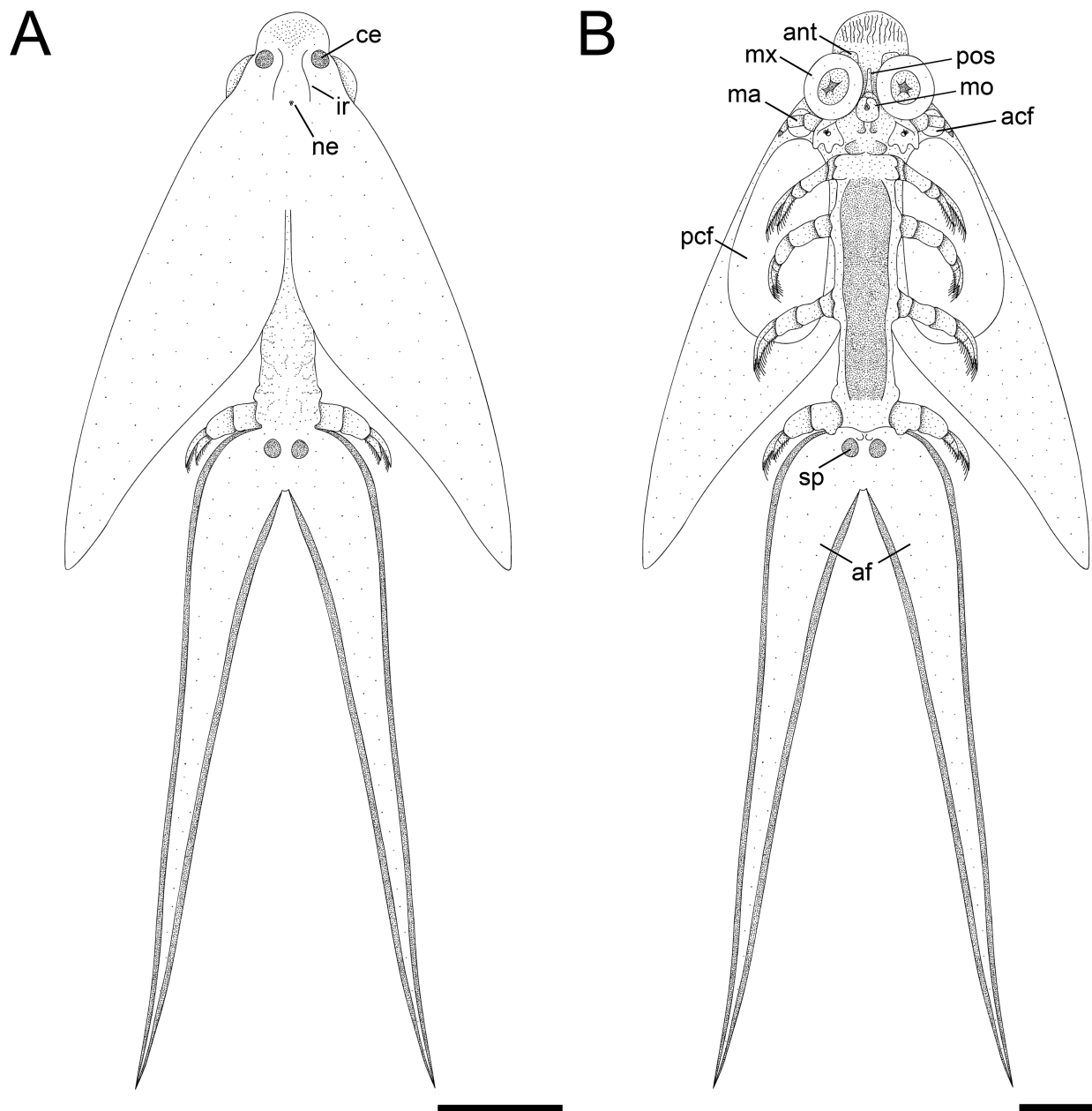


FIGURE 2. *Dipteropeltis longicaudatus* sp. nov., adult holotype (MUSM 5128, specimen I.2). (A) Dorsal view. (B) Ventral view. Abbreviations: acf = anterior carapace field, af = abdomen field, ant = antenna, ce = compound eye, ir = interocular rod, ma = maxilla, mo = mouth, mx = maxillule, ne = nauplius eye, pcf = posterior carapace field, pos = pre-oral spine, sp = spermatheca. Scale bars = 2 mm.

Dipteropeltis Calman, 1912

Dipteropeltis longicaudatus sp. nov.

Etymology. Species name *longicaudatus* means “long-tailed” in Latin. The gender is masculine.

Type material. Type specimens and vouchers were deposited in the Helminthological Collection of the Museum of Natural History at the San Marcos University (MUSM) in Lima, Peru: holotype MUSM 5128 (adult specimen I.2); paratypes MUSM 5129 (adult specimen I.3) and MUSM 5130 (juvenile specimen II.5).

Type locality. Tahuayo River, Maynas, Loreto, Peru (-4.394542, -73.264189).

Type host. *Triportheus albus*.

Adult morphology

(Group I; description based on holotype (MUSM 5128, specimen I.2). Measurements taken from right side of specimen.)

(Figs. 2–5, Suppl. Fig. 2)

The head shield of *Dipteropeltis longicaudatus* sp. nov is flat and semicircular. Laterally at the base of the shield are two compound eyes visible dorsally and ventrally. A pair of interocular rods run sagittally between the compound eyes and around a single nauplius eye. A dark green triangular region is found anterior to the rods (Fig. 3C). On the underside of the head shield, distinct ridges run sagittally.

The antennae and antennules (Fig. 5A) are partially obscured by the maxillulae (Fig. 2B). Antennae are moderately sized (~325 µm) and have six segments sparsely covered in setae (Fig. 5A). Antennules are smaller (~240 µm) and bi-segmented, branching to seven elongate setae at the distal end. The maxillulae are circular, with their diameter ranging from 0.8 to 1.0 mm, representing an average of 5.4% of the total lengths of the adult specimens (Table 1). The rim of the maxillule is divided into three zones (Fig. 4B). Zone 1 (interior section) has rows of folded membrane which become more apparent along the interior margin. Zone 2 (middle section) is widest, containing three rows of round sclerites (diameter 10–12 µm). Zone 3 (exterior section) is flat. A pre-oral spine is apparent in specimens I.2 (Fig. 2B) and I.7 (Fig. 4A). The spine was not clearly visible in some specimens. The mouth (Fig. 4C) is located between the maxillulae and below the spine. The labrum has an inverted U-shape and extends down to become the lateral protrusions. These obscure the base of the mandibles, which cross over the labial spines. The labium is large and extends over the labrum, creating a circular opening to the mouth.

Maxillae are uniramous and six-segmented (Fig. 5B). Proximal segment 1 is roughly equilaterally triangular, and the caudal side has three blunt protrusions. Remaining segments extend laterally then curl posteriorly into a C-shape. Segments 2–5 cylindrical, sequentially smaller. Segment 1 with uniramous scales grouped along anterior margin. Several setae grouped in center of this segment, pointing ventrally from body surface. Segments 2–4 moderately covered in pectinate scales. Segment 5 lacking scales, segment 6 with two small spines.

Carapace lobes approximately 6.8 cm long extending from behind the head shield past abdomen base (Fig. 2A). Midgut within thoracic region branching laterally from main ducts running along the median. Vessels branch within the carapace lobes. Two carapace fields on anteroventral portion of both carapace lobes (Fig. 2B). Anterior fields small and circular (0.47 mm x 0.48 mm), posterior fields large, oval-shaped (1.53 mm x 3.37 mm). Fields slightly lighter than surrounding tissue in some specimens.

Eggs can be identified by their circular shape within the lower cephalothorax. Gravid specimens are dark orange in that region of the body (Fig. 3B). Non-gravid specimens range from light orange to white.

Legs (Figs. 2B, 5C) distally biramous. Distance between each pair of legs is 0.5 mm. In leg 1, the precoxa is 73 µm, the coxa is 405 µm, the basipodite is 178 µm, the unsegmented endopodite is 292 µm, and the exopodite is 568 µm. In leg 2, the precoxa is 199 µm, the coxa is 373 µm, the basipodite is 243 µm, the bi-segmented endopodite is 312 µm, and the exopodite is 487 µm. In leg 3, the precoxa is 187 µm, the coxa is 357 µm, the basipodite is 268 µm, the bi-segmented endopodite is 422 µm, and the exopodite is 620 µm. In leg 4, the precoxa is 324 µm and contains the natatory lobe, the coxa is 316 µm, the basipodite is 97 µm, the bi-segmented endopodite is 315 µm, and the exopodite is 466 µm. All legs have plentiful filamentous setae on both endopodite and exopodite.

Abdominal lobes extend beyond the length of the carapace lobes, averaging 62% of the total length of the specimens (Table 1). The split of the abdominal lobe averages 88% of the entire length of the abdominal lobe (Table 1). Abdominal lobes taper to a fine point. Much of the dorsal cephalothorax and abdomen is faint green or white in

specimens. Specimens have fields along the interior ventral surface of the abdominal lobes (Fig. 4E). The external boundaries of these fields can be easily identified by a difference in pigmentation, which is dark in some specimens (nearly mahogany), and lighter in others (faint orange) (Figs. 3A, B). The main portion of the abdominal lobes is typically light green to white.

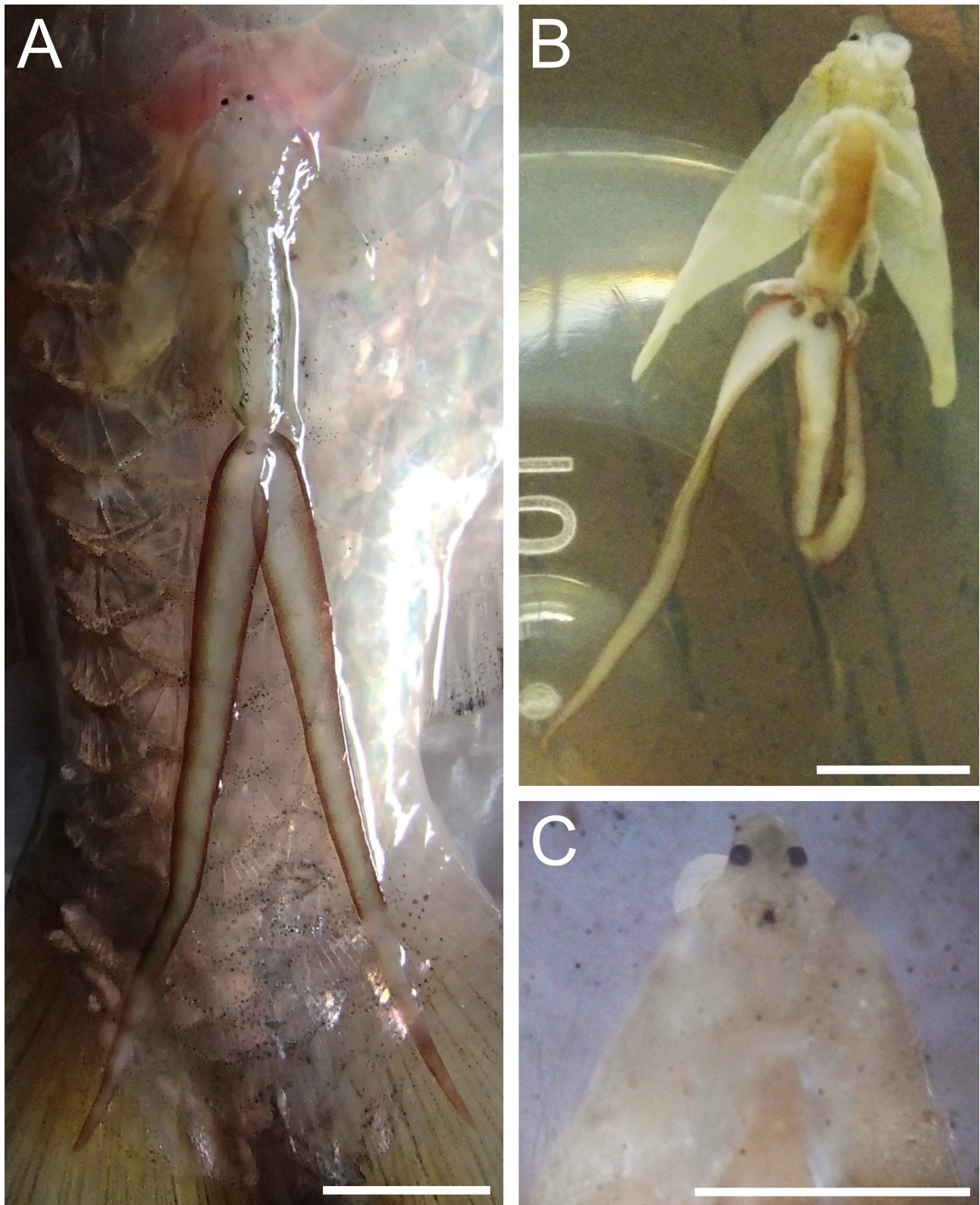


FIGURE 3. *Dipteropeltis longicaudatus* sp. nov. adult specimens. (A) Specimen I.4 attached to host *Triportheus albus*, dorsal view. (B) Specimen I.2 (holotype MUSM 5128) preserved in 70% isopropyl alcohol, ventral view (missing right maxillule). (C) Specimen I.4, dorsal view of head and carapace. All scale bars = 5 mm.

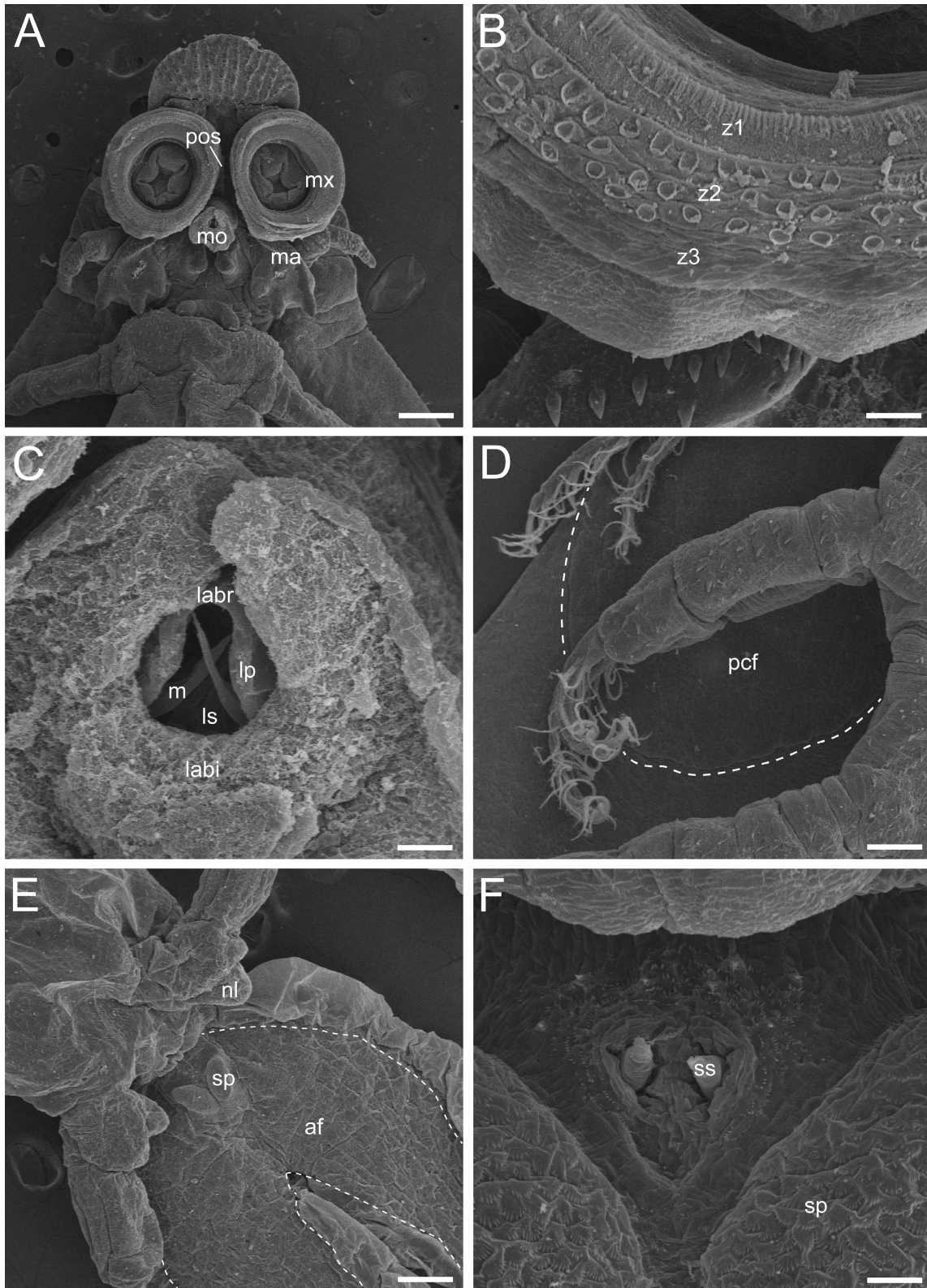


FIGURE 4. *Dipteropeltis longicaudatus* sp. nov. adult specimens I.7 (A–D, F) and I.4 (E), scanning electron micrographs. (A) Ventral view. (B) Sucker rim showing zones (z1–3). (C) Mouth. (D) Spacing shown between legs and partial outline of posterior carapace field. (E) Partial abdomen field, fourth pair of legs, and spermathecae. (F) Spermathecal spines. Abbreviations: af = abdomen field, labi = labium, labr = labrum, lp = lateral protrusion, ls = labial spines, m = mandible, ma = maxilla, mo = mouth, mx = maxillule, nl = natatory lobe, pcf = posterior carapace field, pos = pre-oral spine, sp = spermatheca, ss = spermathecal spines. Dashed lines represent border of thin integument of pcf (D) and af (E). Scale bars: A = 300 μ m, B = 30 μ m, C = 20 μ m, D = 150 μ m, E = 300 μ m, F = 20 μ m.

At the anterior end of the abdomen, paired ovoid spermathecae are visible, heavily covered in pectinate scales (Fig. 4F). Spermathecae are darker than the surrounding tissue. Anteromedially paired spermathecal spines are surrounded by numerous coarse scales (Fig. 4F). Furcal rami are absent.

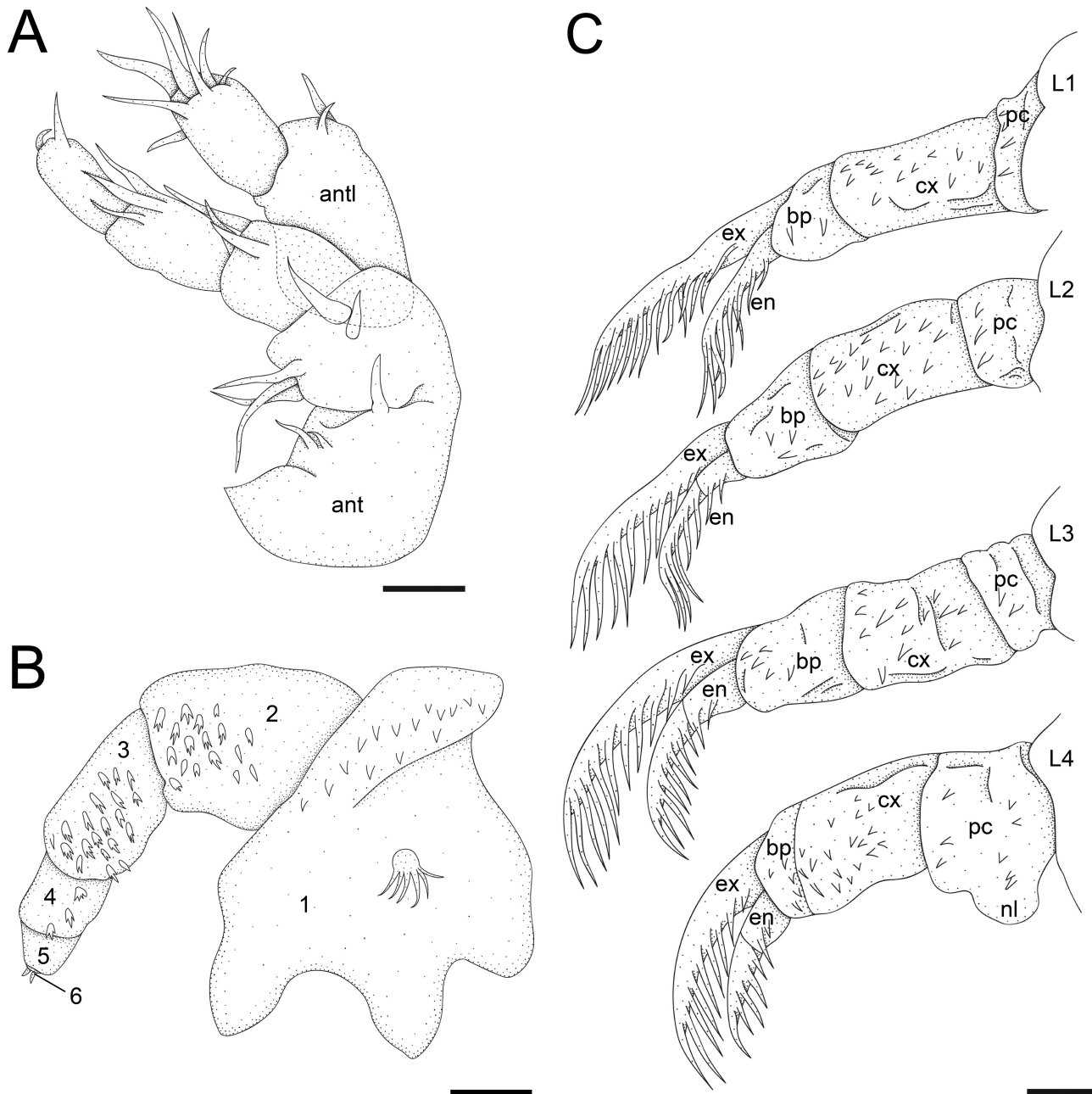


FIGURE 5. *Dipteropeltis longicaudatus* sp. nov., adult holotype (MUSM 5128, specimen L2) structures in ventral view. (A) Right antenna and antennule. (B) Right maxilla. (C) Right legs 1–4. Abbreviations: 1 = first segment, 2 = second segment, 3 = third segment, 4 = fourth segment, 5 = fifth segment, 6 = sixth segment, ant = antenna, antl = antennule, bp = basipodite, cx = coxa, en = endopodite, ex = exopodite, L1 = first leg, L2 = second leg, L3 = third leg, L4 = fourth leg, nl = natatory lobe, pc = precoxa. Scale bars: A = 50 μ m, B = 100 μ m, C = 150 μ m.

Juvenile morphology

(Group II; description based on paratype (MUSM 5130, specimen II.5). Measurements taken from right side of specimen.)

(Figs. 6–8)

Like adult specimens, the head shield is semicircular with two compound eyes (though larger in relation to body size in juveniles), as well as two interocular rods, a single nauplius eye, and a green triangular region anteromedial to the compound eyes. The ventral head shield has the same ridges as in adults, but hornlike projections are also apparent (Fig. 8D).

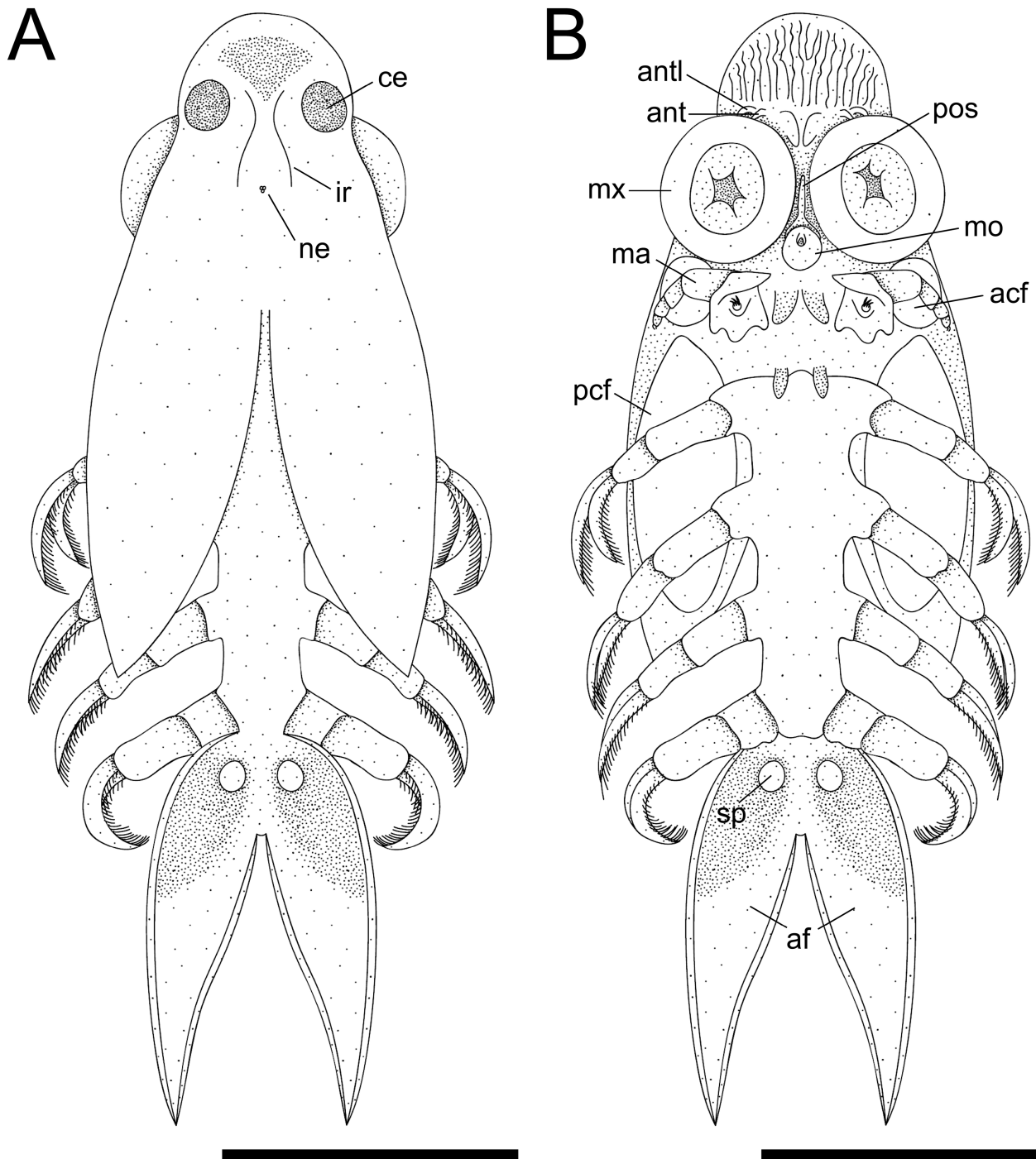


FIGURE 6. *Dipteropeltis longicaudatus* sp. nov., juvenile paratype (MUSM 5130, specimen II.5). (A) Dorsal view. (B) Ventral view. Abbreviations: acf = anterior carapace field, af = abdomen field, ant = antenna, antl = antennule, ce = compound eye, ir = interocular rod, ma = maxilla, mo = mouth, mx = maxillule, ne = nauplius eye, pcf = posterior carapace field, pos = pre-oral spine, sp = spermatheca. Scale bars = 1 mm.

Antennae are moderately sized (~120 μm) and have six segments sparsely covered in setae (Figs. 5A, 8D). Antennules are smaller (~90 μm) and bi-segmented, branching to seven elongate setae at the distal end. The rims of the maxillulae are also divided into three zones, with more defined features than in the adult specimens (Fig. 8B). Zone 1 (interior section) has 1–2 rows of denticles (4 μm) pointing outward. Zone 2 (middle section) is widest, containing three distinct rows of round sclerites (diameter 6 μm). Zone 3 (exterior section) is mostly flat, lined interiorly with a single row of pectinate bristles (6 μm). A partially retracted pre-oral spine was visible in specimen II.6. The same oral structures are present as in the adult, but the labium has a slightly different morphology (Fig. 8C). The maxillae resemble those of the adult with no notable differences (Figs. 5B, 8E).

Carapace lobes do not extend past the abdominal lobes (Fig. 6A). Carapace fields resemble those of the adult, with a circular anterior region (0.19 mm x 0.24 mm) and an ovoid posterior region (0.35 mm x 0.93 mm) (Fig. 6B). These fields are light in color and surrounded by heavy pigmentation on the lateral sides (Fig. 7B). Eggs are not visible in any juvenile specimens, although some have a light orange coloration in the lower cephalothorax.

Legs follow the same structure as those of the adults but have less space between them anteroposteriorly, <0.5 mm (Figs. 6B, 8A). The natatory lobes are visible but diminutive.

Borders of the fields on the abdomen are not as distinct as in adults. Abdominal lobes are notably shorter than those of the adults, on average only 29% of the total body length (Table 1). The split of the abdominal lobe averages 74% of the entire length of the abdominal lobe (Table 1). Lobes are more lanceolate in shape than in the adults.

Spermathecae are usually white surrounded by tissue ranging in color from mahogany to bright green. They are less developed and not well visible under light or scanning electron microscopy, but spermathecal spines are apparent (Fig. 8F). Scales and furcal rami are absent.

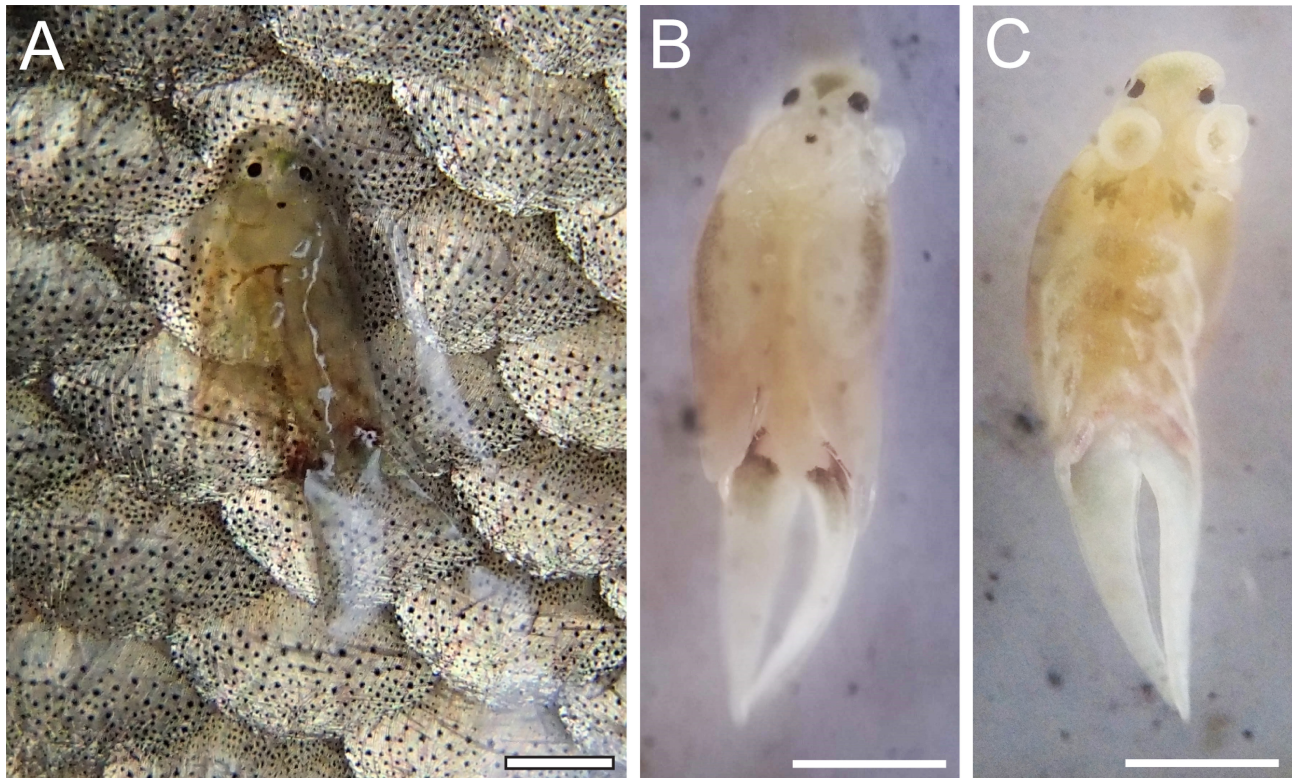


FIGURE 7. *Dipteropeltis longicaudatus* sp. nov. juvenile specimen II.3. (A) Attached to host *Brycon amazonicus*, dorsal view. (B) Dorsal view. (C) Ventral view. All scale bars = 1 mm.

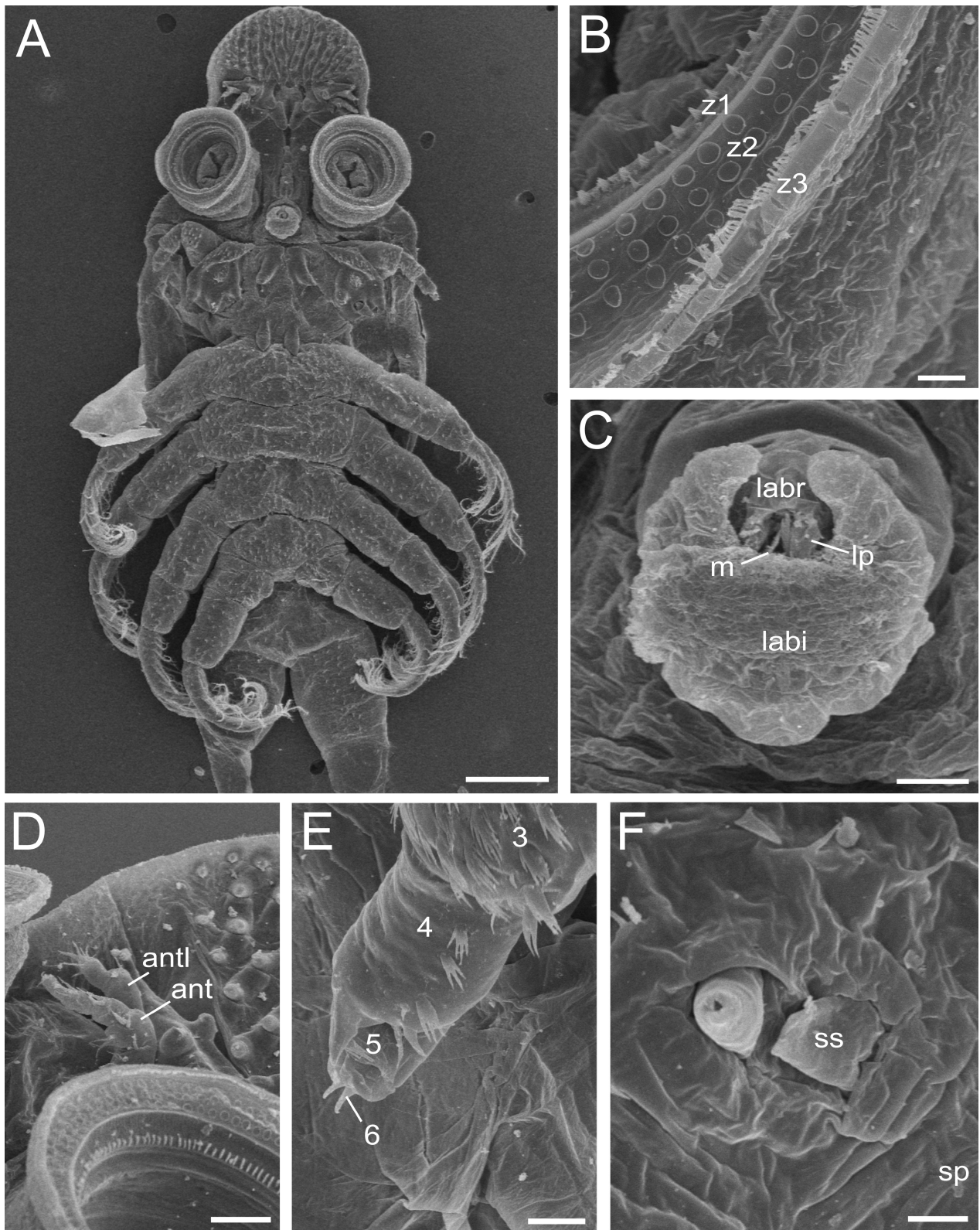


FIGURE 8. *Dipteropeltis longicaudatus* **sp. nov.** juvenile specimen II.6, scanning electron micrographs. (A) Ventral view. The distances between legs here are smaller cf. Fig. 6B due to shrinkage during preservation. (B) Sucker rim showing zones (z1–3). (C) Mouth (labial spines are not visible from this view). (D) Antennae and antennule. Hornlike projections of ridges visible at top right. (E) Distal end of right maxilla, showing segments 3–6. (F) Spermathecal spines. Abbreviations: 3 = third segment, 4 = fourth segment, 5 = fifth segment, 6 = sixth segment, ant = antennae, antl = antennule, labi = labium, labr = labrum, lp = lateral protrusion, m = mandible, sp = spermatheca, ss = spermathecal spines. Scale bars: A = 300 μ m, B = 15 μ m, C = 30 μ m, D = 50 μ m, E = 20 μ m, F = 10 μ m.

Family Argulidae Leach, 1819

Dipteropeltis Calman, 1912

Dipteropeltis hirundo

Group III consisted of a single gravid adult individual of *D. hirundo* (Suppl. Fig. 3). Measurements and ratios are similar to the averages of previously published *D. hirundo* specimens in Neethling *et al.* 2014. HC/HA for the current specimen was found to be 1.09, compared to the prior average of 1.22. HA/HC was 0.92 cf. 0.86, CSL/HC was 0.75 cf. 0.85, ASL/AL was 0.85 cf. 0.81, AL/HA was 0.35 cf. 0.42, AL/HC was 0.32 cf. 0.35, SD/HA was 0.05 cf. 0.05, and SD/HC was 0.05 cf. 0.04. This specimen, similar to other recorded *D. hirundo* specimens, has an asymmetrical head in which the maxillulae are not directly next to each other (Neethling *et al.* 2014, Møller & Olesen 2010). The left maxillule is set more anterior to the right one, making the head shield extend further forward on the left side (Suppl. Fig. 3).

Barcoding

Sequences for the COI DNA barcoding region were obtained from one specimen within each of the three groups. For each specimen, template DNA produced an amplicon of the correct size (658 bp). There was no sequence variation in the COI sequences of specimens I.1 and II.4, suggesting that these specimens are conspecific. The COI sequence for specimen III.1 (*D. hirundo*) was most similar (81.8%) to *Dolops* sp. DQ889096.1 downloaded from GenBank, and was 76.2% similar to both specimens I.1 and II.4. Sequences for specimens I.1 and II.4 were ~65–80% similar to reference sequences for species of *Argulus*, *Chonopeltis*, and *Dolops* downloaded from GenBank. Comparison of *D. longicaudatus* **sp. nov.** COI sequences to those of a majority of other argulid species for which reference sequences are available indicates that the *D. longicaudatus* **sp. nov.** sequences are distinct, and sister to *Dipteropeltis hirundo* and *Dolops* sp. (Suppl. Fig. 1). BOLD accession number for *D. longicaudatus* **sp. nov.** adult I.1 is FLMO81-23, for *D. longicaudatus* **sp. nov.** juvenile II.4 is FLMO80-22, and for *D. hirundo* adult III.1 is FLMO82-23.

Behavior

Dipteropeltis spp. collected for this study were first observed attached to their host. *Triportheus albus* (Triportheidae) represents a new host species and family for *Dipteropeltis* spp. Prevalence of *Dipteropeltis* spp. on hosts was 28%, and no more than one specimen was attached per host. We observed *Dipteropeltis* spp. using their maxillule suction discs to attach caudolaterally to their teleost hosts (Fig. 3A), while the carapace and abdomen in both groups could be seen rhythmically contracting at 1 second intervals (Suppl. Videos 1, 2).

The use of the maxillule suction discs to slowly “walk” along a surface was observed in one of the adult specimens. This specimen was observed ventrally, attached upside down to a clear plastic surface via both maxillulae. It would release one maxillule and extend it further to one side, reattaching it. It would then release the other maxillule and move it closer to the first one. The process would then repeat (Suppl. Video 3). This behavior was not observed in juvenile individuals.

Some adult specimens took up to 30 minutes to detach from their host, while others had to be manually removed. Once detached, adults made minimal movements and were not apt to swim. However, juvenile specimens all detached independently within a few minutes of their host being caught, then moved freely in the water using their legs. Swimming motion was erratic and characterized by short bursts with minor pauses in between (Suppl. Video 4). Adult specimens would also move their legs rhythmically after detaching, however, this motion did not seem to aid in movement (Suppl. Video 3).

Discussion

Dipteropeltis is a poorly described genus—not just taxonomically and geographically, but also ontogenetically, genetically, and behaviorally. Accordingly, we characterize a new species and compare it with the two other

known species of *Dipteropeltis*. Morphological differences were observed (Suppl. Table 1) that indicate that *D. longicaudatus* **sp. nov.** is a unique taxon of *Dipteropeltis*. The most salient feature of *D. longicaudatus* **sp. nov.** are the elongate abdominal lobes of the adult female specimens, which represent on average 62% of the total body length (AL/HA, Table 1) cf. 42% in *D. hirundo* and 48% in *D. campanaformis* (Neethling *et al.* 2014). Similar to *D. campanaformis*, *D. longicaudatus* **sp. nov.** specimens' abdominal lobes extend beyond the carapace lobes; however the carapace lobes are chevron-shaped. Another diagnostic feature is the elongate maxillae, which curve more posterolaterally than those of *D. hirundo* and especially *D. campanaformis* (Fig. 5B; Neethling *et al.* 2014). The first segment is also unique in that it is trilobed on the posterior side and has several setae protruding from the center. The second segment is more slender than that of the other two species, and the remaining segments are more similar to *D. hirundo*. Additional differences include the mouth, which is not flush with the surrounding tissue as in *D. campanaformis* and is not as conelike as those of *D. hirundo* (Neethling *et al.* 2014). Setae on the endopodites and exopodites of both juveniles and adults are more numerous than those of both *D. hirundo* and *D. campanaformis*.

Molecular analysis reveals that the two COI sequences derived from *D. longicaudatus* **sp. nov.** are identical to each other, indicating that the specimens are indeed conspecific. Results also indicate that *D. longicaudatus* **sp. nov.** is distinct and not conspecific with any similar species for which reference COI sequences are available. However, our ability to compare the *D. longicaudatus* **sp. nov.** sequences to other species is limited by the availability of reference sequences. GenBank accessioned, publicly accessible COI sequences are available for only 12 of the ~200 species of *Argulus*, *Chonopeltis*, and *Dolops*. No COI sequences for any *Dipteropeltis* species are available, and we were only able to compare *D. longicaudatus* **sp. nov.** sequences to that of the *D. hirundo* specimen collected sympatric to the *D. longicaudatus* **sp. nov.** specimens. Availability of reference sequences from additional argulid species would better resolve the distinctness of the sequences derived from *D. longicaudatus* **sp. nov.** specimens. Furthermore, the COI sequence tree (Suppl. Fig. 1) should not be interpreted as a phylogeny, as such results cannot elucidate evolutionary relationships above the species level. However, these molecular data combined with morphological data support the recognition of *D. longicaudatus* **sp. nov.** as a distinct species. Therefore, we conclude that the two groups detailed in this paper are adult (Group I) and juvenile (Group II) female *D. longicaudatus* **sp. nov.**

Spermathecae of juvenile specimens are not as pronounced nor coated in scales like in adults. They are usually lighter in color. Presence of spermathecae in juvenile specimens is not surprising, as *Argulus* spp. are described to have seven to ten developmental stages and spermathecae become visible during the second stage of *Argulus foliaceus* (Rushton-Mellor & Boxshall 1994). There is an absence of accessory copulatory structures such as a peg-and-socket mechanism or spermatophores as found in other branchiurans (Avenant-Oldewage & Swanepoel 1993; Avenant-Oldewage & Van As 1990), further supporting the conclusion that all these specimens are female.

Adult and juvenile *D. longicaudatus* **sp. nov.** have similar head shields and mouth cones. Maxillae and maxillulae of both groups are nearly identical, apart from minor differences in the zones along the rim of the suckers. Legs 1–3 are similar in both groups; the natatory lobe on leg 4 is larger in adults. Juveniles have smaller abdominal lobes, representing 29% of the total body length on average. The average abdomen split lengths are large in both, 88% of the abdomen length in adults and 74% of the abdomen length in juveniles (ASL/AL, Table 1). The carapace lobes in *D. longicaudatus* **sp. nov.** are triangular in shape, making up an average of 55% (HC/HA, Table 1) of the entire body length in adult specimens. This value is 71% in juvenile specimens (HC/HA, Table 1). As a percentage of carapace lobe length, the average carapace split length is 71% for adults and 48% for juveniles (CSL/HC, Table 1).

The body length of most branchiurans is typically 3–5mm (Suárez-Morales 2020), although *D. hirundo* and *Dolops longicauda* Heller, 1857 have been reported up to 26–30mm long (Neethling *et al.* 2014; Heller 1857; Møller 2009). Thus, with a total length of 31.5mm, *D. longicaudatus* **sp. nov.** specimen I.4 represents the longest branchiuran documented to date (Fig. 3A, Table 1). Most of this length is the abdomen, and this gravid specimen had the longest absolute (22.0mm AL) as well as relative (0.70 AL/HA) abdomen lengths of all the specimens (Table 1). It should also be noted that the extremely elongate abdominal lobes of *D. longicaudatus* **sp. nov.** adults are similar to those of *Dolops longicauda* described from Brazil (Heller 1857; Suppl. Fig. 4). These long lobes may have evolved convergently as a functional adaptation to similar environmental conditions.

Thorell (1864) coined subclass Branchiura as “gill-tails”, referring to the seemingly respiratory function of the ventral fields on the abdominal lobes, which was later supported by Leydig (1889), Bernecker (1909), and others. However, it was later suggested that similar fields within the carapace function primarily for osmoregulation (Haase 1975a,b; Debaisieux 1953). These fields are covered with thinner integument than the surrounding carapace and contain a high density of blood vessels underneath, allowing for ease of ion exchange between the branchiuran and

its environment. Here, we presume that the similar-looking integument in the anterior carapace and abdomen fields serves a similar purpose in respiration and/or maintaining a proper ion balance, with the caveat that future research may better elucidate the function(s) of these three fields. Having larger fields, such as those in the elongate abdomen, would allow these animals to intake more gases and/or ions from their surrounding water. For example, Fryer (1968) noted elongate abdominal lobes with thin integument in *Chonopeltis schoutedeni* Brian, 1940, purportedly to increase the area for respiration, since this species parasitizes bottom-dwelling hosts where the current is not as strong as at the surface. *D. longicaudatus* **sp. nov.** was collected in a blackwater river, a type which has much lower oxygen content and ionic concentrations than whitewater rivers (Janzen 1974). Furthermore, the Tahuayo River floods throughout the entire length of its banks for part of the year (Coomes 1992), while the river is nearly dry during the rest of the year. Due to this fluctuation, ion content in the water is expected to vary drastically.

Thus, we hypothesize that the pulsating behavior is related to such respiratory and/or osmotic exchange (Suppl. Videos 1, 2). In addition, an adult specimen was observed attached to a surface via their maxillulae, but still moving its legs briskly. Despite not moving, this behavior continued for the duration of the attachment. Fryer (1968) suggests that this movement aids in water flow over the fields within the carapace and abdomen. It is possible that the elongate carapace of *Dipteropeltis* spp. also aids in swimming (Van As & Van As 2019). While juvenile specimens appear to rely solely on their legs for movement (Suppl. Video 4), adult specimens seem too large to be easily propelled by their legs, which become relatively smaller as their overall size increases. The legs could generate a minute amount of forward momentum, and the carapace lobes could act as a plane's wings, allowing the parasite to "soar" through the water while expending less energy. The suction disc "walking" behavior (Suppl. Video 3) is presumably one mechanism that enables the parasite to move around on its host. Such behavior may be present in other argulids, although *Dolops* spp. have hooks instead of suction discs and are still able to move around on the host (Van As & Van As 2019).

The adult and juvenile specimens of *D. longicaudatus* **sp. nov.** herein provide new insights into this relatively obscure genus of fish parasites. Ultimately, more research is needed to fully understand the physiology, life history, and diversity of these organisms as well as their role in the neotropical ecosystem.

Acknowledgements

We would like to thank Dr. Paul Beaver and Amazonia Expeditions' Amazon Research Center for providing access to the Tamshiyacu Tahuayo Reserve in which specimens could be collected, as well as equipment that was used to initially study specimens. We are grateful for the assistance that Dr. Clare Dennison provided with SEM imaging and analysis. We appreciate Candelaria Domingo, Alex Urlaub, and Lilyanna Lopez for technical assistance with molecular work. In Fig. 1, the Peru map is provided under CC BY-SA 3.0 license by Wikimedia Commons user Urutseg, the globe inset is provided under CC BY-SA 3.0 license by Wikimedia Commons user Addicted04, and the map inset panel is provided under CC BY 4.0 by Google Maps.

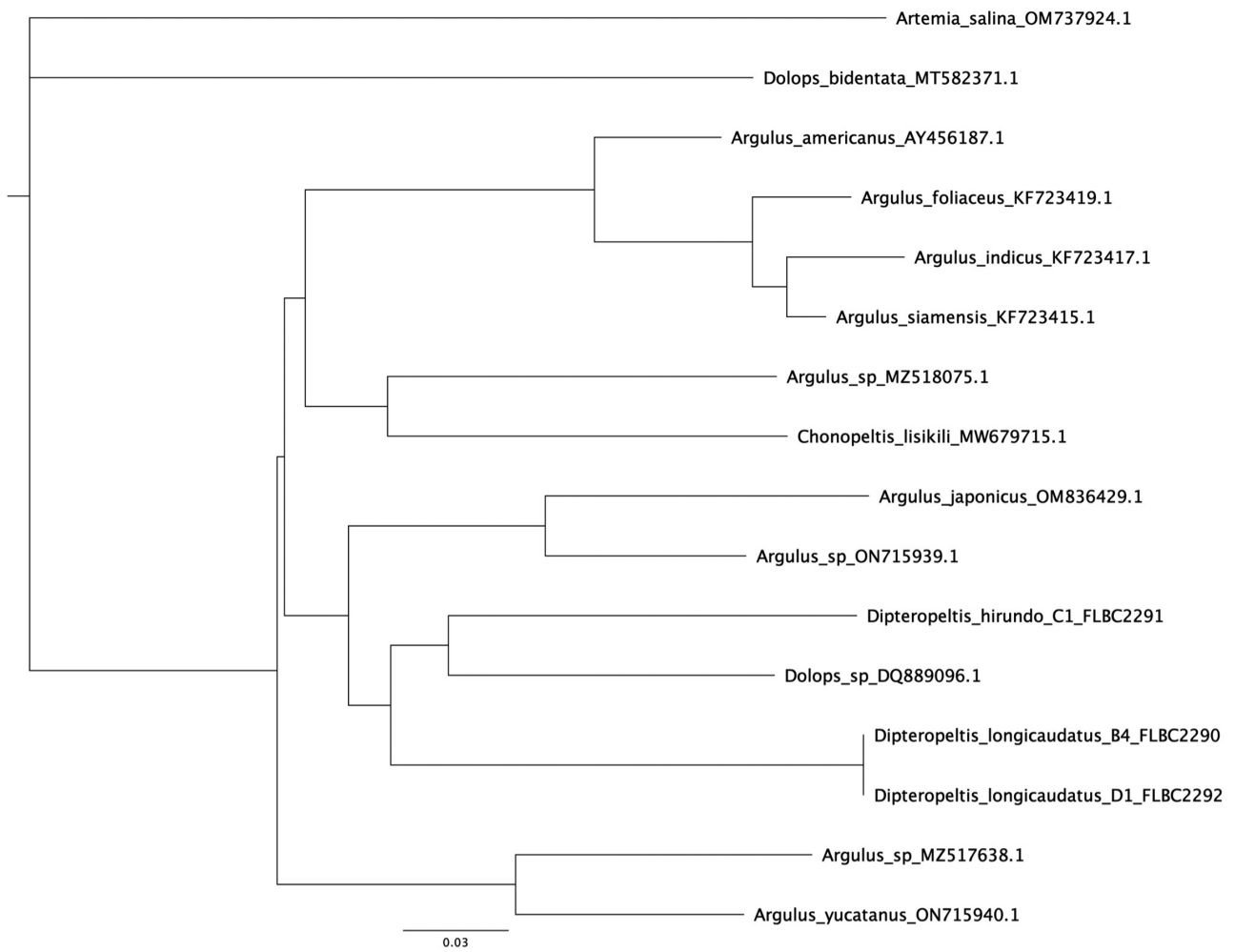
References

- Avenant-Oldewage, A. & Swanepoel, J.H. (1993) The male reproductive system and mechanism of sperm transfer in *Argulus japonicus* (Crustacea: Branchiura). *Journal of morphology*, 215 (1), 51–63.
<https://doi.org/10.1002/jmor.1052150104>
- Avenant-Oldewage, A. & Van As, J.G. (1990) On the reproductive system of *Dolops ranarum* (Stuhlmann, 1891) (Crustacea: Branchiura). *African Zoology*, 25 (1), 67–71.
<https://doi.org/10.1080/02541858.1990.11448191>
- Bernecker, A. (1909) Zur Histologie der Respirationsorgane bei Crustaceen. *Zoologische Jahrbücher. Abteilung für Anatomie und Ontogenie der Tiere*, 27, 583–630. [in German]
- Calman, W.T. (1912) On *Dipteropeltis**, a New Genus of the Crustacean. Order Branchiura. *In Proceedings of the Zoological Society of London*, 82 (4), 763–766.
<https://doi.org/10.1111/j.1469-7998.1912.tb07553.x>
- Carvalho, L.N., Del-Claro, K. & Takemoto, R.M. (2003) Host-parasite interaction between branchiurans (Crustacea: Argulidae) and piranhas (Osteichthyes: Serrasalminae) in the Pantanal wetland of Brazil. *Environmental Biology of Fishes*, 67 (3), 289–296.
<https://doi.org/10.1023/A:1025899925545>

- Coomes, O.T. (1992) Blackwater rivers, adaptation, and environmental heterogeneity in Amazonia. *American Anthropologist*, 94 (3), 698–701.
<https://doi.org/10.1525/aa.1992.94.3.02a00120>
- de Oliveira, R.C., Santos, M.D.C.F., Bernardino, G., Hrbek, T. & Farias, I.P. (2018) From river to farm: an evaluation of genetic diversity in wild and aquaculture stocks of *Brycon amazonicus* (Spix & Agassiz, 1829), Characidae, Bryconinae. *Hydrobiologia*, 805 (1), 75–88.
<https://doi.org/10.1007/s10750-017-3278-0>
- Debaisieux, P. (1953) Histologie et histogénèse chez *Argulus foliaceus* L. (Crustacé, Branchiure). *Cellule*, 55, 1–53. [in French]
- Folmer, O., Black, M., Hoeh, W., Lutz, R. & Vrijenhoek, R. (1994) DNA primers for amplification of mitochondrial cytochrome c oxidase subunit I from diverse metazoan invertebrates. *Molecular Marine Biology and Biotechnology*, 3, 294–299.
- Fontana, M., Takemoto, R.M., Malta, J.C.D.O. & Mateus, L.A.D.F. (2012) Parasitism by argulids (Crustacea: Branchiura) in piranhas (Osteichthyes: Serrasalminae) captured in the Caiçara bays, upper Paraguay River, Pantanal, Mato Grosso State, Brazil. *Neotropical Ichthyology*, 10, 653–659.
<https://doi.org/10.1590/S1679-62252012005000019>
- Fryer, G. (1968) The parasitic Crustacea of African freshwater fishes; their biology and distribution. *Journal of Zoology*, 156 (1), 45–95. [1987]
<https://doi.org/10.1111/j.1469-7998.1968.tb08578.x>
- Haase, W. (1975a) Ultrastruktur und Funktion der Carapaxfelder von *Argulus foliaceus* (L.) (Crustacea, Branchiura). *Zeitschrift für Morphologie der Tiere*, 81 (4), 161–189. [in German]
<https://doi.org/10.1007/BF00301154>
- Haase, W. (1975b) Ultrastrukturelle Veränderungen der Carapaxfelder von *Argulus foliaceus* L. in Abhängigkeit vom Ionengehalt des Lebensraums (Crustacea, Branchiura). *Zeitschrift für Morphologie der Tiere*, 81 (4), 343–353. [in German]
<https://doi.org/10.1007/BF00298492>
- Hadfield, K.A. (2019) History of discovery of parasitic crustacea. In: Smit, N., Bruce, N., Hadfield, K. (Eds.), *Parasitic Crustacea. Vol. 3. Zoological Monographs*. Springer, Cham, pp. 7–71.
https://doi.org/10.1007/978-3-030-17385-2_2
- Hadfield, K.A. & Smit, N.J. (2019) Parasitic crustacea as vectors. In: Smit, N., Bruce, N. & Hadfield, K. (Eds.), *Parasitic Crustacea. Vol. 3. Zoological Monographs*. Springer, Cham, pp. 331–342.
https://doi.org/10.1007/978-3-030-17385-2_7
- Heller, C. (1857) Beiträge zur Kenntniss der Siphonostomen. *Sitzungsberichte der Kaiserlichen Akademie der Wissenschaften, Mathematisch-Naturwissenschaftliche Classe*, 25, 89–108. [in German]
- Janzen, D.H. (1974) Tropical blackwater rivers, animals, and mast fruiting by the Dipterothripidae. *Biotropica*, 6 (2), 69–103.
<https://doi.org/10.2307/2989823>
- Leach, W.E. (1819) Entomostracés, Entomostraca. *Dictionnaire des Sciences Naturelles*, 14, 524–543. [in French]
- Leydig, F. (1889) Ueber *Argulus foliaceus*. *Archiv für Mikroskopische Anatomie*, 33 (1), 1–51. [in German]
<https://doi.org/10.1007/BF02956022>
- Luque, J.L., Pavanelli, G., Vieira, F., Takemoto, R. & Eiras, J. (2013) Checklist of Crustacea parasitizing fishes from Brazil. *Check List*, 9 (6), 1449–1470.
<https://doi.org/10.15560/9.6.1449>
- Mamani, M., Hamel, C. & Van Damme, P.A. (2004) Ectoparasites (Crustacea: Branchiura) of *Pseudoplatystoma fasciatum* (surubi) and *P. tigrinum* (chuncuina) in Bolivian white-water floodplains. *Ecología en Bolivia*, 39 (2), 9–20.
- Mennerat, A., Nilsen, F., Ebert, D. & Skorping, A. (2010) Intensive farming: evolutionary implications for parasites and pathogens. *Evolutionary biology*, 37 (2), 59–67.
<https://doi.org/10.1007/s11692-010-9089-0>
- Mikheev, V.N., Pasternak, A.F. & Valtonen, E.T. (2015) Behavioural adaptations of argulid parasites (Crustacea: Branchiura) to major challenges in their life cycle. *Parasites & Vectors*, 8 (1), 1–10.
<https://doi.org/10.1186/s13071-015-1005-0>
- Møller, O.S. & Olesen, J. (2010) The little-known *Dipteropeltis hirundo* Calman, 1912 (Crustacea, Branchiura): SEM investigations of paratype material in light of recent phylogenetic analyses. *Experimental Parasitology*, 125 (1), 30–41.
<https://doi.org/10.1016/j.exppara.2009.09.008>
- Møller, O.S. (2009) Branchiura (Crustacea)-survey of historical literature and taxonomy. *Arthropod Systematics & Phylogeny*, 67 (1), 41–55.
- Møller, O.S., Olesen, J., Avenant-Oldewage, A., Thomsen, P.F. & Glenner, H. (2008) First maxillae suction discs in Branchiura (Crustacea): development and evolution in light of the first molecular phylogeny of Branchiura, Pentastomida, and other “Maxillopoda”. *Arthropod structure & development*, 37 (4), 333–346.
<https://doi.org/10.1016/j.asd.2007.12.002>
- Molnár, L.K., Székely, C. (1998) Occurrence of Skrjabillanid nematodes in fishes of Hungary and in the intermediate host, *Argulus foliaceus*. *Acta Vet Hung*, 46 (4), 451–463.
- Moravec, F., Vidal-Martínez, V. & Aguirre-Macedo, L. (1999) Branchiurids (*Argulus*) as intermediate hosts of the daniconematid nematode *Mexiconema cichlasomae*. *Folia Parasitol*, 46 (1), 79.

- Neethling, L.A.M., Malta, J.C.D.O. & Avenant-Oldewage, A. (2014) Additional morphological information on *Dipteropeltis hirundo* Calman, 1912, and a description of *Dipteropeltis campanaformis* n. sp. (Crustacea: Branchiura) from two characiform benthopelagic fish hosts from two Northern rivers of the Brazilian Amazon. *Zootaxa*, 3755 (2), 179–193. <https://doi.org/10.11646/zootaxa.3755.2.4>
- Poly, W.J. (2008) Global diversity of fishlice (Crustacea: Branchiura: Argulidae) in freshwater. *Hydrobiologia*, 595 (1), 209–212. <https://doi.org/10.1007/s10750-007-9015-3>
- Ratnasingham, S. & Hebert, P.D.N. (2007) BOLD: the Barcode of Life Datasystem (<http://www.barcodinglife.org>). *Molecular Ecology Notes*, 7, 355–364. <https://doi.org/10.1111/j.1471-8286.2007.01678.x>
- Ringuelet, R. (1943) Revisión de los Argúlidos Argentinos (Crustácea, Branchiura) Con el catálogo de las especies Neotropicales. *Revista del Museo de La Plata (Nueva Serie)*, 3, 43–99. [in Spanish]
- Rushton-Mellor, S. K. & Boxshall, G.A. (1994) The developmental sequence of *Argulus foliaceus* (Crustacea: Branchiura). *Journal of Natural History*, 28 (4), 763–785. <https://doi.org/10.1080/00222939400770391>
- Sanger, F., Nicklen, S. & Coulson, A.R. (1977) DNA sequencing with chain-terminating inhibitors. *Proceedings of the National Academy of Sciences of the United States of America*, 74, 5463–5467. <https://doi.org/10.1073/pnas.74.12.5463>
- Smallbone, W., Van Oosterhout, C. & Cable, J. (2016) The effects of inbreeding on disease susceptibility: *Gyrodactylus turnbulli* infection of guppies, *Poecilia reticulata*. *Experimental Parasitology*, 167, 32–37. <https://doi.org/10.1016/j.exppara.2016.04.018>
- Suárez-Morales, E. (2020) Class Branchiura. In: Rogers, D.C., Damborenea, C. & Thorp, J. (Eds.), *Thorp and Covich's Freshwater Invertebrates*. Academic Press, Cambridge, pp. 797–807. <https://doi.org/10.1016/B978-0-12-804225-0.00022-8>
- Thorell, T. (1864) Om tvenne europeiske Argulider; jemte anmärkningar om Argulidernas morfologi och systematiska ställning, samt en öfversigt af de för närvarande kända arterna af denna familj. *Öfversigt af de Kungliga Vetenskaps-Akademiens Förhandlingar*, 1, 7–72. [in Swedish]
- Van As, J.G.V. & Van As, L.L. (2019) Adaptations and types of crustacean symbiotic associations. In: Smit, N., Bruce, N. & Hadfield, K. (Eds.), *Parasitic Crustacea. Vol. 3*. Zoological Monographs, Springer, Cham, pp. 135–178. https://doi.org/10.1007/978-3-030-17385-2_4
- Weibezahn, F.H. & Cobo, T. (1964) *Seis argulidos* (Crustacea, Branchiura) parasitos de peces dulce-acuicolas en Venezuela, con descripción de una nueva especie del genero *Argulus*. *Acta Biologica Venezuelica*, 4 (2), 119–144. [in Spanish]

Supplementary Materials



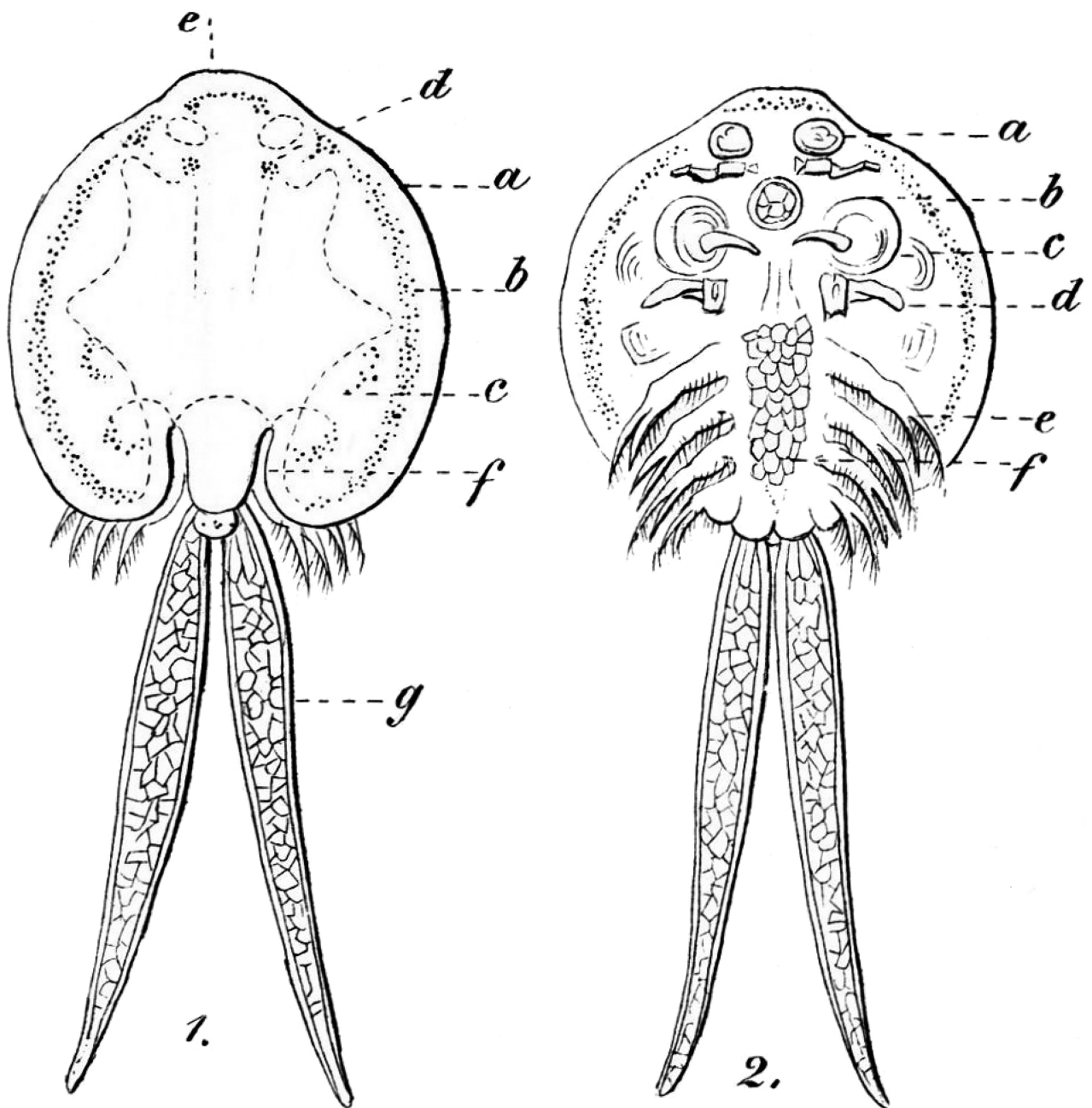
SUPPLEMENTARY FIGURE 1. Neighbor-joining tree of our specimens of *Dipteropeltis longicaudatus* **sp. nov.** (juvenile and adult) and *D. hirundo*, along with related branchiurans and one branchiopodan outgroup (brine shrimp *Artemia salina*). Tree was constructed based on a 533 bp fragment of the barcoding region of the cytochrome c oxidase subunit I gene. The two *D. longicaudatus* **sp. nov.** sequences had 100% similarity with each other, and 76.2% similarity with *D. hirundo*. The scale bar represents the expected number of nucleotide substitutions per site.



SUPPLEMENTARY FIGURE 2. Adult *Dipteropeltis longicaudatus* sp. nov. attached to hosts.



SUPPLEMENTARY FIGURE 3. *Dipteropeltis hirundo* (specimen III.1) attached to host *Brycon amazonicus* at the base of the caudal fin. Note overlap of carapace lobes and dark branching ducts of the midgut.



SUPPLEMENTARY FIGURE 4. Elongate abdominal lobes (g) in *Dolops longicauda* (Heller 1857, Plate I).

SUPPLEMENTARY TABLE 1. Direct comparison among adult *Dipteropeltis (D.) campanaformis*, *D. hirundo*, and *D. longicaudatus* **sp. nov.** Columns for the former two species have been reproduced from Neethling *et al.* 2014.

Feature	<i>D. campanaformis</i>	<i>D. hirundo</i>	<i>D. longicaudatus</i>
Head shield	Square Narrower than maxillules No folds	Round Wider than maxillules Folded	Semicircular Narrower than maxillules Folded
Carapace lobes	Elliptical Bell-shaped Covers anterior portion of abdomen dorsally Average ratio 84.05% of body length (HA)	Straight Swallow-shaped Covers length of abdomen dorsally Average ratio 122.07% of body length (HA)	Triagonal Chevron-shaped Does not cover any part of abdomen Average ratio 54.71% of body length (HA)
Carapace fields	Anterior triangular oval Posterior ovoid	Anterior oval Posterior ovoid with concave ridge on anterior edge	Anterior circular Posterior ovoid
Mouth	Round, labium encircles labrum Recessed on cephalon	Labium and labrum joined laterally Projected on siphon-like cone	Round, flat labium encircles labrum Projected on cylindrical cone
Pre-oral structure	Diminutive and triangular, no duct or spine	Elongated eversible sheath, spine present	Elongated eversible sheath, spine present
Maxillules	Zone 1: lined radiating rows of micro-papillae Zone 2: suctorial plates Zone 3: 2 rows of elongate concentric parallel discoidal scales Average ratio 5.0% of total length (HA)	Zone 1: folds in an erratic pattern Zone 2: rounded sclerites with minute setules arranged within Zone 3: thin cuticle and a brush-border Average ratio 4.1% of total length (HC)	Zone 1: folds in an erratic pattern Zone 2: rounded sclerites Zone 3: thin, flat cuticle Average ratio 5.4% of total length (HA)
Maxillae	Conical Two round protrusions covered by pectinate scales medially on segment three and four	Hooked, distal three segments folded at an angle to basal three segments No protrusions	Segments curve to form C-shape Trilobed on posterior side of segment one
Natatory lobes	Equally bilobed	Elongate and rounded with a basal protrusion	Blunt, rounded
Abdomen	Furcal rami not observed Lanceolate tips Average ratio 47.8% of total length (HA)	Furcal rami present Blunt tips Average ratio 35.55% of total length (HC)	Furcal rami not observed Elongate, lanceolate tips Average ratio 61.57% of total length (HA)
Spermathecal area	Sparsely scattered with course pectinate scales	Numerous course pectinate scales	Numerous course pectinate scales

Supplementary Materials. The following supporting information can be downloaded at the DOI landing page of this paper.

SUPPLEMENTARY VIDEO 1. *Dipteropeltis longicaudatus* **sp. nov.**: video of adult specimen I.4 attached to host *Triportheus albus*, showing pulsating abdomen fields.

SUPPLEMENTARY VIDEO 2. *Dipteropeltis longicaudatus* **sp. nov.**: video of juvenile specimen II.5 attached to host *Brycon amazonicus*, showing pulsating abdomen fields.

SUPPLEMENTARY VIDEO 3. *Dipteropeltis longicaudatus* **sp. nov.**: video of adult specimen I.6 employing alternating suction disc “walking” movement along a surface. Four “strides” from eight sequences of release and reattachment. Leg movement is also employed, presumably to encourage water current over the carapace fields.

SUPPLEMENTARY VIDEO 4. *Dipteropeltis longicaudatus* **sp. nov.**: video of two specimens; adult I.7 is stationary, but juvenile II.6 is seen rapidly swimming around in the water.